

Resummation of fermionic in-medium ladder diagrams to all orders

N. Kaiser

Physik-Department T39, Technische Universität München, D-85747 Garching, Germany

email: nkaiser@ph.tum.de

Abstract

A system of fermions with a short-range interaction proportional to the scattering length a is studied at finite density. At any order a^n , we evaluate the complete contributions to the energy per particle $\bar{E}(k_f)$ arising from combined (multiple) particle-particle and hole-hole rescatterings in the medium. This novel result is achieved by simply decomposing the particle-hole propagator into the vacuum propagator plus a medium-insertion and correcting for certain symmetry factors in the $(n - 1)$ -th power of the in-medium loop. Known results for the low-density expansion up to and including order a^4 are accurately reproduced. The emerging series in ak_f can be summed to all orders in the form of a double-integral over an arctangent function. In that representation the unitary limit $a \rightarrow \infty$ can be taken and one obtains the value $\xi = 0.5067$ for the universal Bertsch parameter. We discuss also applications to the equation of state of neutron matter at low densities and mention further extensions of the resummation method.

PACS: 05.30.Fk, 12.20.Ds, 21.65+f, 25.10.Cn

1 Introduction and summary

Dilute degenerate many-fermion systems with large scattering lengths are of interest e.g. for modeling the low-density behavior of nuclear or neutron star matter. Also dilute systems of ultracold atoms can nowadays be trapped. Because of the possibility to tune (magnetically) atomic interactions through so-called Feshbach resonances, ultracold fermionic gases provide an exceptionally valuable tool to explore the (non-perturbative) many-body dynamics at weak and strong coupling together with the transition from the superconducting to the Bose-Einstein condensed state. Of particular interest in this context is the so-called unitary limit in which the two-body interaction has the critical value to support a boundstate at zero energy. In that special situation the s-wave scattering length diverges, $a \rightarrow \infty$, and the (strongly) interacting many-fermion system becomes scale invariant. Its groundstate energy is then determined by a single universal number, the so-called Bertsch parameter ξ , which measures the ratio of the energy per particle, $\bar{E}(k_f)^{(\infty)}$, to that of a free Fermi gas, $\bar{E}(k_f)^{(0)} = 3k_f^2/10M$. Here, k_f denotes the Fermi momentum and M stands for the (heavy) fermion mass.

The calculation of ξ is an intrinsically non-perturbative problem which has been approached in recent years by numerical quantum Monte-Carlo simulations (in a periodic box). As the state of the art, at present a value of $\xi \simeq 0.38$ seems to emerge from these calculations [1], presumably with still debatable error bars due to finite-size corrections etc. The equation of state of neutron matter at low densities has also been studied using quantum Monte-Carlo techniques [2, 3]. Due to the very large neutron-neutron scattering length, $a_{nn} \simeq 19$ fm, neutron matter at low densities, $\rho_n = k_f^3/3\pi^2 \leq 0.05$ fm³, is supposed to be a fermionic gas close to the unitarity limit. The results of a variety of sophisticated many-body calculations are summarized in Figs. 3,4 of ref. [3] and these give indications for a value of $\xi_{nn} \approx 0.5$.

On the other hand effective field theory methods have been used to rederive and systematically improve the low-density expansion for a system of fermions with short-range interactions

[4, 5, 6]. In particular, effective range corrections and (logarithmic) contributions from three-particle scattering have been included. In an unpublished paper, Steele [7] has computed several higher order contributions proportional to $(ak_f)^3$ and $(ak_f)^4$. These are generated either by multiple particle-particle and hole-hole rescatterings in the medium or they arise from particle-hole ring diagrams. Based on some numerical evidence, Steele argued that in the limit of large space-time dimensions D the hole-hole contributions would be suppressed. Under this assumption the resummation of the particle-particle contributions becomes possible (in the limit $D \rightarrow \infty$) in the form of a simple geometrical series: $-(2ak_f/3\pi)[1 + 2ak_f/\pi]^{-1}$. (We are choosing the sign-convention such that a positive scattering length $a > 0$ corresponds to attraction.) The Bertsch parameter following from Steele's approximation is $\xi^{(\text{St})} = 4/9$, surprisingly close to recent quantum Monte-Carlo results. The validity of Steele's arguments concerning the expansion in $1/D$ has been critically reassessed in the more elaborate work by Schäfer et al. [8]. There it has been shown that if the strong coupling limit $a \rightarrow \infty$ is taken after the limit $D \rightarrow \infty$ the universal Bertsch parameter is $\xi^{(\infty)} = 1/2$ (see eq.(44) in ref. [8]).

Moreover, the particle-particle ladders (for $D = 4$) have been resummed in ref. [8] in the form of a phase space integral over a geometrical series, $-a[1 + ak_f F_{pp}(s, \kappa)/\pi]^{-1}$, and the corresponding Bertsch parameter had the (rather small) value $\xi^{(pp)} \simeq 0.24$. In the same paper an analogous expression for the sum of all hole-hole ladders has been given (see eq.(25) in ref. [8]). In that case the geometrical series involves two subtractions (hole-hole ladders start to contribute at order a^3) and the unitary limit $a \rightarrow \infty$ does not exist for this term. The same feature applies to the sum of all particle-hole ring diagrams, which have been discussed in section IV of ref. [8]. Beyond these partial resummation results there exist still large classes of diagrams with mixed particle-particle and hole-hole ladders which have not been considered in ref. [8] (or elsewhere in the literature). Clearly, these should all be resummed in order to see whether they contribute in the limit $a \rightarrow \infty$ to the universal Bertsch parameter ξ . The first mixed (pp and hh) ladder appears at order a^4 and it has been considered by Steele [7]. Hammer et al. [9] have carefully checked Steele's calculation (for $D = 4$) and they find differences for just this term. In particular, the numerical value given for it in eq.(16) of ref. [7] (middle term) has to be corrected and multiplied by a factor 2. Actually, Hammer et al. [9] find a simpler analytical representation for it in the form of a phase space integral over the squared particle-particle bubble times the hole-hole bubble, $3F_{pp}^2(s, \kappa)F_{pp}(-s, \kappa)$ (see eq.(7) in section 3). Besides this leading term, results for mixed particle-particle and hole-hole ladders at higher orders $a^n, n \geq 5$ are not known. For large n their classification and combinatorial counting is already a non-trivial problem.

The purpose of the present paper is to close this gap. We will evaluate, at any order a^n , the complete contributions to the energy per particle $\bar{E}(k_f)$ arising from combined (multiple) particle-particle and hole-hole rescatterings in the medium. A key to the solution of this problem is a different organization of the many-body calculation from the start. Instead of treating (propagating) particles and holes separately, we keep them together and measure the difference to the propagation in vacuum by a "medium-insertion". The latter involves a delta-function for on-shell kinematics and a step-function which restricts momenta to the region inside the Fermi sphere. In that organizational scheme the pertinent in-medium loop (or in-medium bubble) is complex-valued. The contribution to the energy per particle $\bar{E}(k_f)$ at order a^n is therefore not obtained directly from the $(n - 1)$ -th power of the in-medium loop. However, after reinstalling the symmetry factors $1/(j + 1)$ which belong to diagrams with $j + 1$ double medium-insertions, a real-valued expression is retained for all n . Known results for the low-density expansion up to and including order a^4 are accurately reproduced in our scheme. The emerging series in ak_f can even be summed to all orders in the form of a double-integral over an arctangent function. In that explicit representation the unitary limit $a \rightarrow \infty$ can be taken straightforwardly and one finds the value $\xi = 0.5067$ for the universal

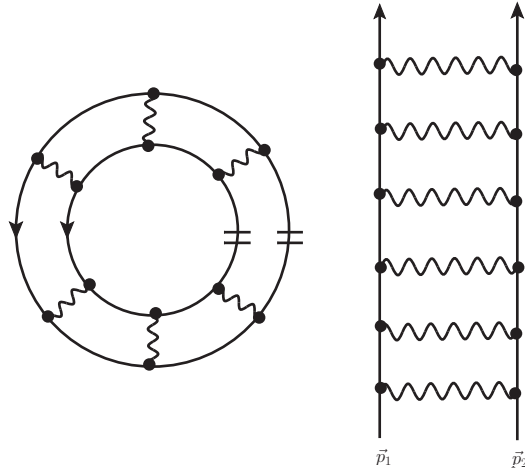


Figure 1: Left: A closed multi-loop diagram with (at least) two medium-insertions representing a contribution to the energy density. Right: After opening at the pair of adjacent medium-insertions (symbolized by short double-lines) the planar ladder diagram results. A wiggly line symbolizes the contact interaction proportional to the scattering length a .

Bertsch parameter. As an application we discuss the equation of state of neutron matter at low densities and finally we mention further possible extensions of the resummation method.

2 Preparation: In-medium propagator

We are interested in the equation of state of a (non-relativistic) many-fermion system with a short-range two-body interaction proportional to the scattering length a . In perturbation theory the interaction contributions to the energy density are represented by closed multi-loop diagrams with a certain number of contact vertices. Their evaluation proceeds via Feynman rules which introduce a factor $4\pi a i/M$ for each interaction vertex and the (non-relativistic) particle-hole propagator:

$$\begin{aligned} G(p_0, \vec{p}) &= i \left(\frac{\theta(|\vec{p}| - k_f)}{p_0 - \vec{p}^2/2M + i\epsilon} + \frac{\theta(k_f - |\vec{p}|)}{p_0 - \vec{p}^2/2M - i\epsilon} \right) \\ &= \frac{i}{p_0 - \vec{p}^2/2M + i\epsilon} - 2\pi \delta(p_0 - \vec{p}^2/2M) \theta(k_f - |\vec{p}|), \end{aligned} \quad (1)$$

for an internal fermion-line carrying energy p_0 and momentum \vec{p} . The (large) fermion mass is denoted by M . The identity in the second line of eq.(1) gives the separation of the in-medium propagator $G(p_0, \vec{p})$ into the vacuum propagator and a “medium-insertion”. Note that by construction a medium-insertion puts a particle onto the mass-shell $p_0 = \vec{p}^2/2M$ and restricts its momentum to the interior of the Fermi sphere $|\vec{p}| < k_f$. The Fermi momentum k_f is related to the density by $\rho = g k_f^3/6\pi^2$. We are considering here only the case with spin-degeneracy factor $g = 2$. Relevant many-body contributions to the energy density come from diagrams with at least two medium-insertions. In case of the closed ladder diagram shown in Fig.1 this minimal pair of medium-insertions has to be placed on adjacent positions of the double-ring, for the following reason. After opening one gets a planar ladder diagram whose energy denominators are all equal to differences of fermion kinetic energies. Only for this planar topology the resulting factors of M (from the energy denominators) will balance the $1/M$ factors from the interaction vertices such that a finite result remains (at each order a^n) in the non-relativistic limit. The open ladder diagram shown in Fig.1 comes in all possible variations with further medium-insertions on internal lines. Due to the momentum-independence of the

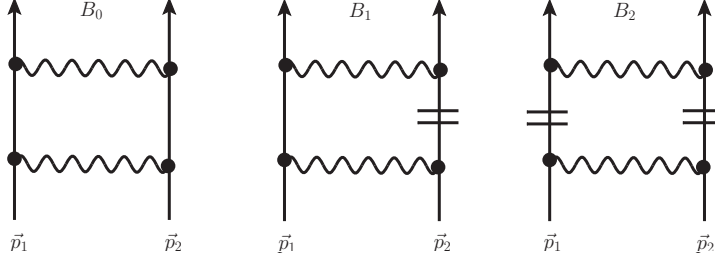


Figure 2: The in-medium loop organized in the number of medium-insertions. The reflected partner of the middle diagram with one medium-insertion is not shown. The external momenta $|\vec{p}_{1,2}| < k_f$ are from the region below the Fermi surface.

contact interaction all these multi-loop diagrams factorize (successive loops have nothing in common) and they can therefore be summed together in the form of a power of the in-medium loop.

3 In-medium loop generated by a contact interaction

The basic ingredient for calculating the energy density arising from ladder diagrams with a short-range contact interaction has been identified as the in-medium loop (or the in-medium bubble). As enforced by the two minimal medium-insertions the incoming momenta \vec{p}_1 and \vec{p}_2 are from the region below the Fermi surface $|\vec{p}_{1,2}| < k_f$. It is convenient to introduce their half sum $\vec{P} = (\vec{p}_1 + \vec{p}_2)/2$ and half difference $\vec{q} = (\vec{p}_1 - \vec{p}_2)/2$. In our ordering scheme the in-medium loop is built up from contributions with zero, one, and two medium-insertions: $B_0 + B_1 + B_2$. The corresponding one-loop diagrams are shown in Fig. 2 and their evaluation is exhibited now in detail.

The contribution B_0 with zero medium-insertions is the well-known rescattering bubble in vacuum. It is normalized relative to the tree-level interaction and therefore it includes only one factor $4\pi a i/M$. The evaluation of the loop integral proceeds as follows:

$$\begin{aligned}
B_0 &= \frac{4\pi a i}{M} \int_{-\infty}^{\infty} \frac{dl_0}{2\pi} \int \frac{d^3 l}{(2\pi)^3} \frac{i}{(\vec{p}_1^2 + \vec{p}_2^2)/4M + l_0 - (\vec{P} + \vec{l})^2/2M + i\epsilon} \\
&\quad \times \frac{i}{(\vec{p}_1^2 + \vec{p}_2^2)/4M - l_0 - (\vec{P} - \vec{l})^2/2M + i\epsilon} \\
&= 4\pi a \int \frac{d^3 l}{(2\pi)^3} \frac{1}{l^2 - \vec{q}^2 - i\epsilon} = \frac{2a}{\pi} \int_0^{\infty} dl \left(1 + \frac{\vec{q}^2}{l^2 - \vec{q}^2 - i\epsilon} \right) = 0 + i a |\vec{q}|, \quad (2)
\end{aligned}$$

using residue calculus for the energy integral $\int_{-\infty}^{\infty} dl_0$ and in the last step the rule $\int_0^{\infty} dl 1 = 0$ of dimensional regularization has been applied. In other regularization schemes the occurring scale-dependent constant $-2\mu/\pi$ is absorbed into a^{-1} to define the renormalized (physical) scattering length [7, 8]. The resummation of infinitely many rescatterings in the vacuum in the form of a geometrical series leads to the unitarized scattering length approximation:

$$f = a \left\{ 1 + ia|\vec{q}| + (ia|\vec{q}|)^2 + \dots \right\} = \frac{1}{a^{-1} - i|\vec{q}|} = \frac{1}{|\vec{q}|(\cot \delta_0 - i)}, \quad (3)$$

which implies the relation $\tan \delta_0 = a|\vec{q}|$ for the s-wave scattering phase shift δ_0 .

Next, we turn to the term B_1 from diagrams with one medium-insertion. There are two equal contributions which differ in their representation merely by the sign of the loop

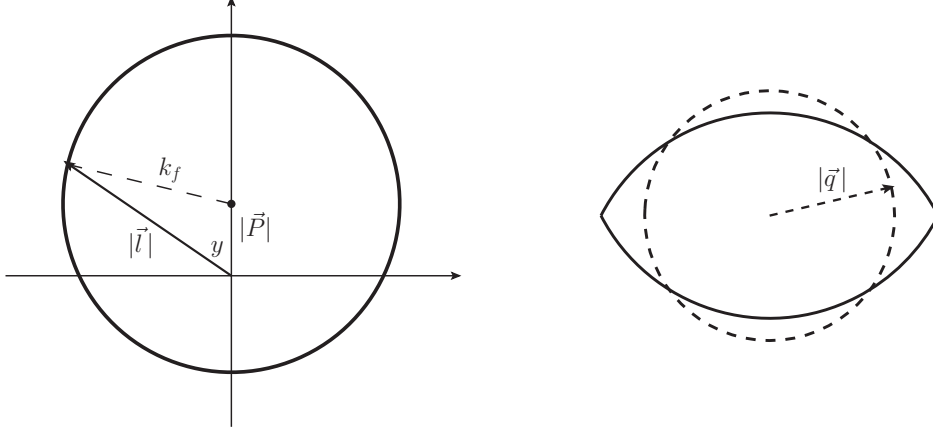


Figure 3: Integration regions in momentum space for the real and imaginary part of the in-medium loop.

momentum \vec{l} and together they read:

$$B_1 = -4\pi a \int \frac{d^3l}{(2\pi)^3} \frac{1}{\vec{l}^2 - \vec{q}^2 - i\epsilon} \left\{ \theta(k_f - |\vec{P} - \vec{l}|) + \theta(k_f - |\vec{P} + \vec{l}|) \right\}. \quad (4)$$

The integral over a shifted Fermi sphere is most suitably performed by using spherical coordinates with the range $0 < |\vec{l}| < |\vec{P}|y + \sqrt{k_f^2 - \vec{P}^2(1 - y^2)}$ of the magnitude $|\vec{l}|$. The quantity y is a directional cosine which covers the full range $-1 < y < 1$ since the displacement vector \vec{P} satisfies the condition $|\vec{P}| < k_f$ (see also the left part of Fig. 3). Carrying out this procedure one obtains the following result for the real part:

$$\text{Re } B_1 = -\frac{ak_f}{\pi} R(s, \kappa), \quad (5)$$

with the logarithmic function:

$$R(s, \kappa) = 2 + \frac{1}{2s} [1 + (s + \kappa)^2] \ln \frac{1 + s + \kappa}{|1 - s - \kappa|} + \frac{1}{2s} [1 + (s - \kappa)^2] \ln \frac{1 + s - \kappa}{1 - s + \kappa}, \quad (6)$$

written in terms of the two dimensionless variables $s = |\vec{p}_1 + \vec{p}_2|/2k_f$ and $\kappa = |\vec{p}_1 - \vec{p}_2|/2k_f$. Since both external momenta $\vec{p}_{1,2}$ are from inside the Fermi sphere one has the additional constraint $s^2 + \kappa^2 < 1$. It is worth to note that the function $R(s, \kappa)$ in eq.(6) is equal to the sum of the particle-particle bubble and the hole-hole bubble, $R(s, \kappa) = F_{pp}(s, \kappa) + F_{pp}(-s, \kappa)$, with the unusual feature that the latter is also taken at momenta below the Fermi surface. For comparison the particle-particle bubble reads [7, 8]:

$$F_{pp}(s, \kappa) = 1 + s - \kappa \ln \frac{1 + s + \kappa}{|1 + s - \kappa|} + \frac{1}{2s} (1 - s^2 - \kappa^2) \ln \frac{|(1 + s)^2 - \kappa^2|}{1 - s^2 - \kappa^2}. \quad (7)$$

Finally, we come to the right diagram in Fig. 2 with two-medium insertions. Obviously, it generates a purely imaginary contribution. The total imaginary part of the in-medium loop has the following representation:

$$\begin{aligned} \text{Im}(B_0 + B_1 + B_2) &= 4\pi a \int \frac{d^3l}{(2\pi)^3} \pi \delta(\vec{l}^2 - \vec{q}^2) \\ &\times \left\{ [1 - \theta(k_f - |\vec{P} - \vec{l}|)] [1 - \theta(k_f - |\vec{P} + \vec{l}|)] \right. \\ &\quad \left. + \theta(k_f - |\vec{P} - \vec{l}|) \theta(k_f - |\vec{P} + \vec{l}|) \right\}, \end{aligned} \quad (8)$$

where we have suitably arranged terms with no, one, and two step-functions $\theta(\dots)$. The first term in eq.(8) of the form $[1 - \theta(\dots)][1 - \theta(\dots)]$ makes no contribution to the imaginary part since the corresponding phase space is completely Pauli-blocked: $2k_f^2 < (\vec{P} - \vec{l})^2 + (\vec{P} + \vec{l})^2 = 2(\vec{l}^2 - \vec{q}^2) + \vec{p}_1^2 + \vec{p}_2^2 < 2k_f^2$. This equation expresses the obvious fact that on-shell scattering of two particles from below the Fermi surface into the region above the Fermi surface is not possible due to energy conservation. Thus there remains the imaginary part due to the second $\theta(\dots)\theta(\dots)$ term in eq.(8). After visualizing the occurring product of θ - and δ -functions one sees that the imaginary part has a nice geometrical interpretation: namely as $|\vec{q}|$ times that part of the solid angle of a (centered) sphere of radius $|\vec{q}|$ which lies inside the intersection region of two spheres of radius k_f with their centers displaced by $2|\vec{P}|$. The corresponding configuration of spheres is sketched in the right part of Fig. 3. After inclusion of the appropriate prefactor the result for the imaginary part of the in-medium loop reads:

$$\text{Im}(B_0 + B_1 + B_2) = \frac{B_2}{2i} = ak_f I(s, \kappa), \quad (9)$$

with the (non-smooth) function:

$$I(s, \kappa) = \begin{cases} \kappa & \text{for } 0 < \kappa < 1 - s, \\ \frac{1}{2s}(1 - s^2 - \kappa^2) & \text{for } 1 - s < \kappa < \sqrt{1 - s^2}, \end{cases} \quad (10)$$

where κ lies in the interval $0 < \kappa < \sqrt{1 - s^2}$. It is interesting to observe that the diagram with two medium-insertions alone gives twice the total imaginary part. Putting the real and imaginary pieces together the complex-valued in-medium loop reads:

$$B_0 + B_1 + B_2 = -\frac{ak_f}{\pi} \left\{ R(s, \kappa) - i\pi I(s, \kappa) \right\}, \quad (11)$$

and if the contribution from the diagram with two medium-insertions is taken out, the imaginary part of that same expression changes sign:

$$B_0 + B_1 = -\frac{ak_f}{\pi} \left\{ R(s, \kappa) + i\pi I(s, \kappa) \right\}. \quad (12)$$

Actually, this special property of the in-medium loop turns out to be crucial in order to derive the correct expression for the energy per particle $\bar{E}(k_f)$ from powers of the (complex-valued) in-medium loop. The derivation of the energy per particle is the topic of the next section.

4 Energy per particle

In this section we show how the contributions to the energy per particle $\bar{E}(k_f)$ at any order a^n can be constructed from the in-medium loop and how the emerging series in ak_f can be summed to all orders. Consider the (open) ladder diagram with n contact interactions. It is given by the $(n - 1)$ -th power of the in-medium loop times a factor $4\pi a i/M$. Closing the two open fermion-lines introduces an integration over the allowed phase space $|\vec{p}_{1,2}| < k_f$. The emerging integrand $(R - i\pi I)^{n-1}$ for the energy density at order a^n would be complex-valued and therefore it cannot yet be the correct one. The deficit of the (naive) iteration method at this intermediate stage becomes evident if one draws all diagrams with (repeated) pairs of adjacent medium-insertions. The corresponding set of diagrams at fourth order a^4 is shown in Fig. 4. These (decorated) diagrams have additional symmetry factors which are not respected by the binomial expansion of $(R - i\pi I)^{n-1} = [(R + i\pi I) + (-2i\pi I)]^{n-1}$. Furthermore, the same symmetry factors correct for the overcounting of certain diagrams as introduced by the terms of the binomial series. As a result of this combinatorial analysis one has to reweight

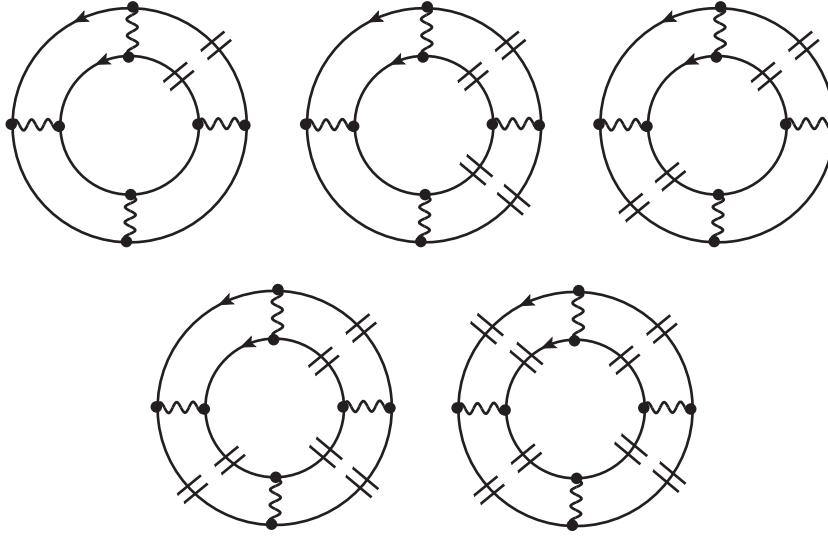


Figure 4: In-medium diagrams contributing to the energy density at order a^4 . Taking into account the proper symmetry factors, their total sum is given by the real-valued expression: $(R + i\pi I)^3 + (R + i\pi I)^2(-2\pi I)(1 + 1/2) + (R + i\pi I)(-2\pi I)^2 + (-2\pi I)^3/4 = R(R^2 - \pi^2 I^2)$. Diagrams with a single medium-insertion on the inner or outer fermion-line between consecutive interactions are not shown.

in the binomial series expansion of $[(R + i\pi I) + (-2i\pi I)]^{n-1}$ the j -th power of $-2i\pi I$ coming from the diagrams with repeated double medium-insertions with the appropriate symmetry factor $1/(j+1)$. This crucial amendment leads to the following summation formula:

$$\sum_{j=0}^{n-1} (R + i\pi I)^{n-1-j} (-2i\pi I)^j \binom{n-1}{j} \frac{1}{j+1} = \frac{1}{2i\pi I n} \{ (R + i\pi I)^n - (R - i\pi I)^n \}. \quad (13)$$

Note that the identity $\binom{n-1}{j}/(j+1) = \binom{n}{j+1}/n$ introduces the binomial coefficients for the n -th power of a sum, and in this way one can easily reproduce the result on the right hand side of eq.(13). In the diagrammatic representation of the energy density, $\binom{n}{j+1}$ is the number of different possibilities to attach $j+1$ double medium-insertions on a ring with n segments and the additional factor $1/n$ comes from the n rotations which transform the ring into itself.

Inspection of the right hand side of eq.(13) shows that the resulting homogeneous polynomials of degree $n-1$ in R and πI are manifestly real for all n . The first five terms read: $n=1$: 1, $n=2$: R , $n=3$: $R^2 - \pi^2 I^2/3$, $n=4$: $R(R^2 - \pi^2 I^2)$, $n=5$: $R^4 - 2R^2\pi^2 I^2 + \pi^4 I^4/5$. In Fig.4 and the appended caption it is shown explicitly how the real-valued expression $R(R^2 - \pi^2 I^2)$ results from the sum of (complex-valued) diagrams once their symmetry factors are taken into account. The same graphology gives at second order a^2 : $(R + i\pi I) + (-2i\pi I)/2 = R$, and at third order a^3 : $(R + i\pi I)^2 + (R + i\pi I)(-2i\pi I) + (-2i\pi I)^2/3 = R^2 - \pi^2 I^2/3$.

At this point we have achieved a representation which includes, at any order a^n , the complete contributions from all mixed particle-particle and hole-hole ladders. One can even go further and sum up the whole series of ladder diagrams to all orders. The pertinent series $\sum_{n=1}^{\infty} [-ak_f(R \pm i\pi I)/\pi]^n/n$ can be solved easily by a (complex) logarithm. After inclusion of the kinetic energy and the Fock exchange-term (which reduces the Hartree term discussed so far by a factor $1 - 1/g = 1/2$) the complete expression for the energy per particle reads:

$$\bar{E}(k_f) = \frac{k_f^2}{2M} \left\{ \frac{3}{5} - \frac{48}{\pi} \int_0^1 ds s^2 \int_0^{\sqrt{1-s^2}} d\kappa \kappa \arctan \frac{ak_f I(s, \kappa)}{1 + \pi^{-1} ak_f R(s, \kappa)} \right\}. \quad (14)$$

The occurring arctangent function refers to the usual branch with odd parity, $\arctan(-x) = -\arctan x$, and values in the interval $[-\pi/2, \pi/2]$. Other branches of the arctangent function are excluded by the weak coupling limit $a \rightarrow 0$, which has to give zero independent of the sign of the scattering length a . Note that there occurs a discontinuity (by an amount $-\pi$) when the denominator passes through zero from positive to negative values. This happens for all positive values of ak_f since the function $R(s, \kappa)$ has a logarithmic singularity at $s = 0$, $\kappa = 1$. The integral-representation for $\bar{E}(k_f)$ given in eq.(14) has some similarity with the expression one obtains from the resummed particle-hole ring diagrams (see eq.(29) in ref. [8]). In that case the arctangent function involves two subtractions (particle-hole ring diagrams start to contribute at order a^3) and the integral extends over a 4-momentum transfer $\int_0^\infty dq_0 \int_0^\infty dq q^2$. In the present case the reduction to a double-integral (over the quarter unit-disc) has been obtained by employing the following master formula for integrals over the interior of two Fermi spheres:

$$\int_{|\vec{p}_{1,2}| < k_f} \frac{d^3 p_1 d^3 p_2}{(2\pi)^6} F(s, \kappa) = \frac{2k_f^6}{\pi^4} \int_0^1 ds s^2 \int_0^{\sqrt{1-s^2}} d\kappa \kappa I(s, \kappa) F(s, \kappa), \quad (15)$$

where $s = |\vec{p}_1 + \vec{p}_2|/2k_f$ and $\kappa = |\vec{p}_1 - \vec{p}_2|/2k_f$. Surprisingly, the imaginary part function $I(s, \kappa)$ defined in eq.(10) occurs here as the pertinent weighting function. Integrals over the outer region of two Fermi spheres can be reduced in a similar way:

$$\begin{aligned} \int_{|\vec{p}_{1,2}| > k_f} \frac{d^3 p_1 d^3 p_2}{(2\pi)^6} F(s, \kappa) \theta(1-s) &= \frac{k_f^6}{\pi^4} \int_0^1 ds s \int_{\sqrt{1-s^2}}^\infty d\kappa \kappa F(s, \kappa) \\ &\times \left[(s^2 + \kappa^2 - 1) \theta(1+s-\kappa) + 2s\kappa \theta(\kappa-1-s) \right]. \end{aligned} \quad (16)$$

This formula is useful e.g. for evaluating the contributions to the energy per particle which arise from multiple hole-hole rescatterings in the medium [7, 8].

5 Expansion in powers of ak_f

Several orders in the low-density expansion of the energy per particle $\bar{E}(k_f)$ are known [4]. The terms stemming from particle-particle and hole-hole ladders can be used as a check of our calculation which is organized differently by not treating separately particles and holes. We find up to and including fourth order:

$$\begin{aligned} \bar{E}(k_f) &= \frac{k_f^2}{2M} \left\{ \frac{3}{5} - \frac{2}{3\pi} ak_f + \frac{4}{35\pi^2} (11 - 2 \ln 2) a^2 k_f^2 \right. \\ &\quad \left. - 0.0755733 a^3 k_f^3 + 0.0524813 a^4 k_f^4 + \dots \right\}. \end{aligned} \quad (17)$$

As it must be, the linear and quadratic coefficients agree analytically. Since only double-integrals are involved the other numerical coefficients can be obtained with high precision. One finds again good agreement with existing calculations [4, 7, 9]. The third order coefficient is: $0.0861836 - 0.0106103 = 0.0640627 + 0.0115106$, where the numbers on the left hand side correspond to our separation $R^2 - \pi^2 I^2/3$ and those on the right side refer to the sum of two-fold particle-particle and two-fold hole-hole rescatterings. The same comparison for the fourth order coefficient gives: $0.0671902 - 0.0147089 = 0.0383116 - 0.0006851 + 6 \cdot 0.0024758$, with our separation $R^3 - R\pi^2 I^2$ versus the sum of triple particle-particle, triple hole-hole, and combined particle-particle and hole-hole scatterings. At this point it is important to note that a factor of 2 is missing in Steele's numerical result for the latter contribution (see middle term in eq.(16) of ref. [7]). This error has been confirmed by Hammer et al. [9] who have carefully

checked Steele's calculation. It has become evident that the squared imaginary part $I(s, \kappa)^2$ of the in-medium loop includes also important many-body correlation effects. Their precise mapping into the (traditional) particle-hole counting scheme is not obvious.

As mentioned in the introduction, Steele [7] has suggested a resummation to all orders in form of a simple geometrical series:

$$\bar{E}(k_f)^{(\text{St})} = \frac{k_f^2}{2M} \left\{ \frac{3}{5} - \frac{2ak_f}{3\pi + 6ak_f} \right\}. \quad (18)$$

Although the original arguments (via a $1/D$ -expansion) have been (partly) invalidated [8], it may serve as a useful reference, in particular since the associated Bertsch parameter $\xi^{(\text{St})} = 4/9$ comes out fairly realistic. We adapt the expansion of the energy per particle in powers of ak_f :

$$\bar{E}(k_f) = \frac{k_f^2}{2M} \left\{ \frac{3}{5} + \sum_{n=1}^{\infty} \frac{c_n}{3} \left(-\frac{2}{\pi} ak_f \right)^n \right\}, \quad (19)$$

such that all coefficients c_n become 1 for Steele's resummation result. Performing the same expansion with our complete expression for $\bar{E}(k_f)$ given in eq.(14) we find the following values for the first dozen expansion coefficients c_n :

$$\begin{aligned} c_1 &= 1, & c_2 &= \frac{3}{35}(11 - 2 \ln 2) = 0.8240319119, \\ c_3 &= \frac{\pi^2}{12} + \frac{9}{160} + \delta c_3 = 0.8787170548, & \delta c_3 &= 2.1365 \cdot 10^{-8}, \\ c_4 &= 1.22717534 - \frac{\pi^2}{70} \left(10 - \pi^2 - 4 \ln^2 2 + \frac{16}{3} \ln 2 \right) = 0.958529, \\ c_5 &= 1.14589, & c_6 &= 1.37081, \\ c_7 &= 1.76240, & c_8 &= 2.19993, \\ c_9 &= 3.03120, & c_{10} &= 3.74458, \\ c_{11} &= 5.85642, & c_{12} &= 5.96732. \end{aligned} \quad (20)$$

One observes that the first few coefficients stay below 1 while the higher ones show a tendency to increase appreciably with n . The apparent region of "convergence" of the power series in ak_f can therefore roughly be estimated as $k_f \leq 1.3/|a|$. Despite various attempts we have not succeeded to derive the exact value of c_3 in terms of (reasonable) mathematical constants. The value $c_3 \simeq \pi^2/12 + 9/160$ represents an extremely accurate analytical approximation, which is far more precise than all previous determinations of this coefficient [4, 7].

For large scattering lengths a the low-density expansion is of very limited validity. In that case one has to take the full expression for the energy per particle $\bar{E}(k_f)$ as given by eq.(14). The solid line in Fig. 5 shows its ratio to the (free) Fermi gas energy $3k_f^2/10M$ as a function of the dimensionless parameter ak_f . The behavior of this ratio is demonstrated for both signs of the scattering length ($a > 0$ for attraction and $a < 0$ for repulsion). Outside the region $k_f|a| > 6$ the curve is almost flat while a sharp peak develops inside with a maximum value of about 1.62 at $ak_f \simeq -0.9$. The dashed curve in Fig. 5 corresponds to Steele's [7] resummation via a geometrical series eq.(18). The behavior on the attractive side ($a > 0$) is quite similar while on the repulsive side ($a < 0$) the artificial pole at $ak_f = -\pi/2$ causes essential differences.

6 Unitary limit

The unitary limit $a \rightarrow \infty$ is of special interest since in this limit the strongly interacting many-fermion system becomes scale invariant. The energy per particle is then determined by

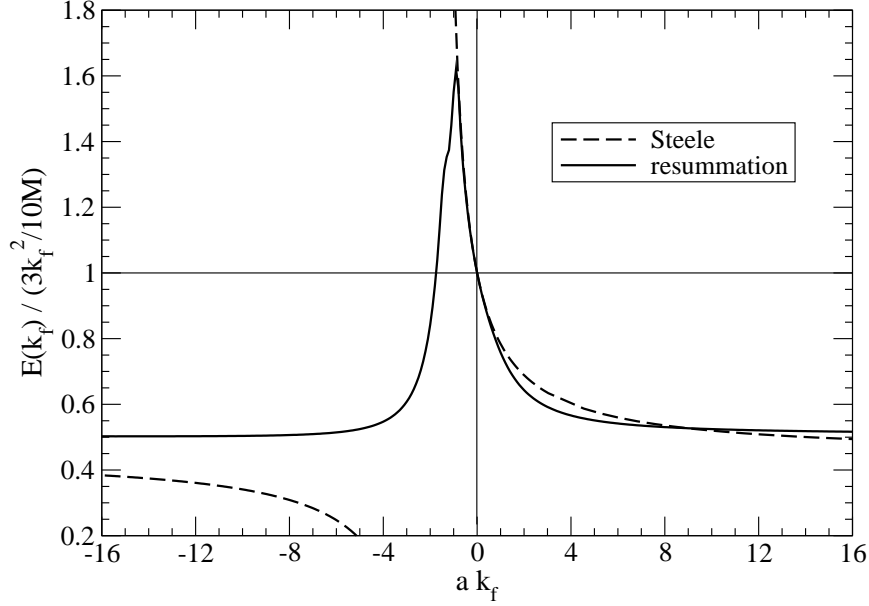


Figure 5: Energy per particle $\bar{E}(k_f)$ divided by the Fermi gas energy $3k_f^2/10M$ as a function of the dimensionless parameter ak_f . An attractive (repulsive) contact interaction corresponds to a positive (negative) value of the scattering length a .

just a constant multiple of the (free) Fermi gas energy:

$$\bar{E}(k_f)^{(\infty)} = \frac{3k_f^2}{10M} \xi, \quad (21)$$

with ξ the so-called Bertsch parameter. Returning to the expression for the energy per particle $\bar{E}(k_f)$ given in eq.(14) one sees that the unitary limit $a \rightarrow \infty$ can be performed straightforwardly. The formula for calculating the Bertsch parameter ξ reads:

$$\xi = 1 - \frac{80}{\pi} \int_0^1 ds s^2 \int_0^{\sqrt{1-s^2}} d\kappa \kappa \arctan \frac{\pi I(s, \kappa)}{R(s, \kappa)} = 0.5067. \quad (22)$$

The resulting numerical value $\xi = 0.5067$ is to be compared with $\xi^{(pp)} \simeq 0.237$ obtained by Schäfer et al. [8] from the resummation of particle-particle ladders. Actually, $\xi^{(pp)}$ is defined by the principal value integral $\xi^{(pp)} = 1 - 80 \int_0^1 ds s^2 \int_0^{\sqrt{1-s^2}} d\kappa \kappa I(s, \kappa) F_{pp}^{-1}(s, \kappa)$ and the necessity to treat the pole-singularity limits the precision in the numerical computation of this number. One observes that the additional mixed particle-particle and hole-hole ladders increase the Bertsch parameter ξ by more than a factor 2. Moreover, the divergence of the subset of hole-hole ladders (for $a \rightarrow \infty$) encountered in ref.[8] has disappeared. Clearly, the value $\xi = 0.5067$ as obtained here via an analytical calculation rooted in perturbation theory is still considerably larger than the result $\xi \simeq 0.38$ from recent quantum Monte-Carlo simulations [1].

In the work by Haussmann et al. [10] a self-consistent, thermodynamically consistent treatment of the unitary Fermi gas at finite temperatures has been presented. In their non-perturbative approach the exact one- and two-particle Green functions serve as an infinite set of variational parameters and extensive numerical work enters into the solutions of the stationarity constraints and the thermodynamical potentials [10]. The resulting Bertsch parameter at zero temperature $T = 0$ was found to be $\xi \simeq 0.36$. This value is remarkably close to the experimental determinations by Bartenstein et al. [11], $\xi = 0.32 \pm 0.11$, and Bourdel et al. [12], $\xi = 0.36 \pm 0.15$.

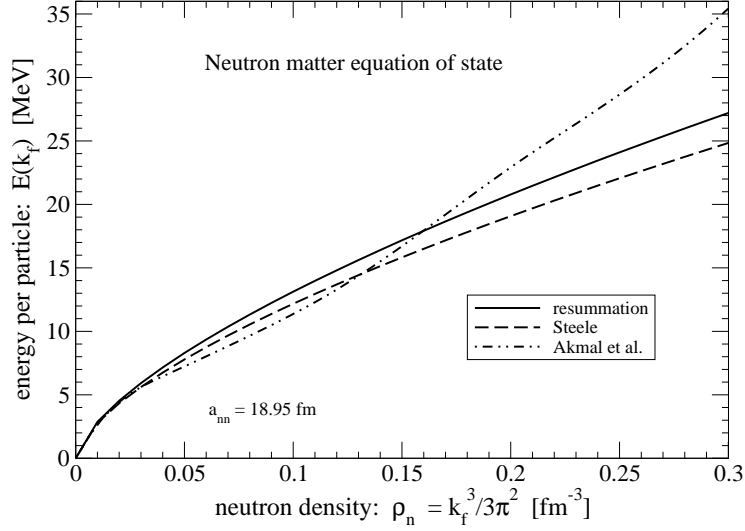


Figure 6: Energy per particle of neutron matter versus the neutron density $\rho_n = k_f^3/3\pi^2$. The dash-dotted line stems from the sophisticated many-body calculation of ref.[15].

7 Application to neutron matter and outlook

As an application of our analytical result eq.(14) for the complete resummation of in-medium ladder diagrams we consider the equation of state of neutron matter. Due to the very large neutron-neutron scattering length $a_{nn} = (18.95 \pm 0.40)$ fm [13, 14] neutron matter at low densities is supposed to be a Fermi gas close to the unitary limit. Recent quantum Monte Carlo simulations [2, 3] based e.g. on the Argonne nucleon-nucleon potential give some indication for such a behavior.

In Fig.6 we show the energy per particle $\bar{E}(k_f)$ of neutron matter as a function of the neutron density $\rho_n = k_f^3/3\pi^2$. The solid line results from our analytical formula eq.(14) inserting $a = a_{nn} = 18.95$ fm for the scattering length and $M = M_n = 939.57$ MeV for the fermion mass. The dash-dotted line corresponds to the sophisticated many-body calculation by the Urbana group [15], to be considered as representative of realistic neutron matter calculations. The dashed line in Fig.6 reproduces Steele's suggestion eq.(18) in the form of a simple geometrical series. One observes good agreement up to rather high neutron densities of $\rho_n \simeq 0.2$ fm $^{-3}$, where the dimensionless parameter $a_{nn}k_f$ reaches values up to $a_{nn}k_f \simeq 34.3$. At higher neutron densities repulsive effects from three-nucleon forces (which are included in the Urbana calculation [15]) start to play a more significant role. The inclusion of the effective range $r_{nn} = (2.75 \pm 0.11)$ fm for s-wave nn -scattering can also lead to sizeable changes in the equation of state, as demonstrated in ref.[16]. Note however, that only the resummed particle-particle ladders have been considered in that work.

Fig.7 shows the neutron matter equation of state in a different representation by plotting the ratio of the energy per particle $\bar{E}(k_f)$ to the (free) Fermi gas energy $3k_f^2/10M$ against the dimensionless parameter $a_{nn}k_f$. The dots in this figure reproduce results of various (quantum Monte-Carlo) calculations of low-density neutron matter and have been taken over from Figs.3,4 in ref.[3] (see original references therein). The solid and dashed curves are the same as in the right part of Fig.5 only continued further out in the parameter ak_f .

The complete resummation of ladder diagrams (with a short-range contact interaction proportional to the s-wave scattering length a) as achieved in this work suggests numerous possible extensions. The s-wave effective range parameter and the p-wave scattering volumes should be included via $\mathcal{O}(p^2)$ terms in the contact interaction. Asymmetries with respect to the spin and/or isospin degrees of freedom can be studied via an appropriate modification of

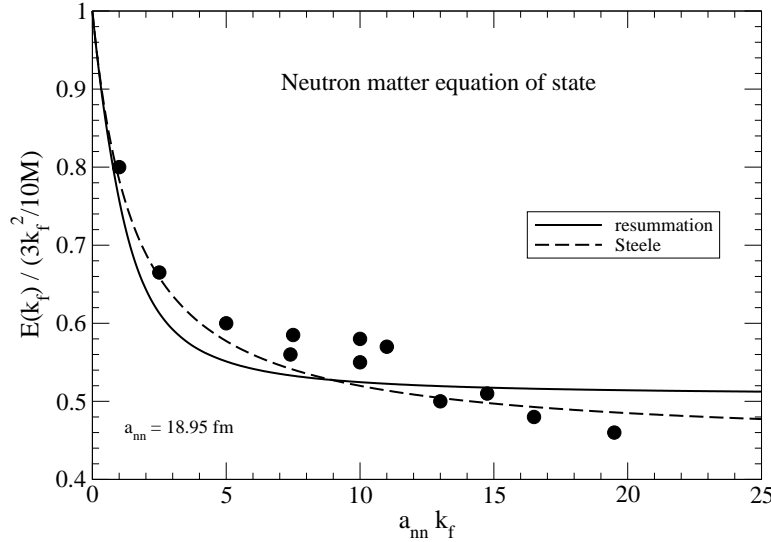


Figure 7: Energy per particle of neutron matter divided by the Fermi gas energy $3k_F^2/10M$. The dots representing various (quantum Monte-Carlo) calculations are taken from ref.[3].

the medium-insertion. The generalization of the resummation method to finite temperatures would be an equally interesting project. Work along these lines in progress.

Acknowledgements

I thank J.W. Holt, A. Schwenk and W. Weise for many useful discussions. I thank H.W. Hammer for communicating to me results from own unpublished work which have been very valuable. This work is partially supported by the DFG Excellence Cluster “Origin and Structure of the Universe”.

References

- [1] M. MacNeil Forbes, S. Gandolfi, A. Gezerlis, “Resonantly interacting fermions in a box”, cond-mat/1011.2197.
- [2] J. Carlson, J. Morales, V.R. Pandharipande, D.G. Ravenhall, *Phys. Rev.* **C68**, 025802 (2003).
- [3] A. Gezerlis, J. Carlson, *Phys. Rev.* **C81**, 025803 (2005).
- [4] H.W. Hammer, R.J. Furnstahl, *Nucl. Phys.* **A678**, 277 (2000).
- [5] R.J. Furnstahl, J.V. Steele, N. Tirfessa, *Nucl. Phys.* **A671**, 396 (2000).
- [6] R.J. Furnstahl, H.W. Hammer, *Ann. Phys. (NY)* **302**, 206 (2002).
- [7] J.V. Steele, “Effective field theory power counting at finite density”, nucl-th/0010066.
- [8] T. Schäfer, C.W. Kao, S.R. Cotanch, *Nucl. Phys.* **A762**, 82 (2005).
- [9] H.W. Hammer et al., unpublished; and private communications.
- [10] R. Haussmann, W. Rantner, S. Cerrito, W. Zwerger, *Phys. Rev.* **A74**, 023610 (2007).
- [11] M. Bartenstein et al., *Phys. Rev. Lett.* **92**, 120401 (2004).
- [12] T. Bourdel et al., *Phys. Rev. Lett.* **93**, 050401 (2004).
- [13] D.E. Gonzales Trotter et al., *Phys. Rev.* **C73**, 034001 (2006).
- [14] Q. Chen et al., *Phys. Rev.* **C77**, 054002 (2008).
- [15] A. Akmal, V.R. Pandharipande, D.G. Ravenhall, *Phys. Rev.* **C58**, 1804 (1998).
- [16] A. Schwenk, C.J. Pethick, *Phys. Rev. Lett.* **95**, 160401 (2005).